

# Optical Parametric Amplification Performance in AsSe<sub>2</sub>-based Hybrid Microstructured Optical Fibers

Hoang Tuan Tong<sup>1</sup>, Kenshiro Nagasaka<sup>1</sup>, Morio Matsumoto<sup>2</sup>, Hiroshige Tezuka<sup>2</sup>, Takenobu Suzuki<sup>1</sup> and Yasutake Ohishi<sup>1</sup>

<sup>1</sup>Research Center for Advanced Photon Technology, Toyota Technological Institute, 2-12-1 Hisakata, Tempaku, Nagoya, 468-8511, Japan

<sup>2</sup>Furukawa Denshi Co., Ltd., 2-3-2, Marunouchi, Chioda-Ku, Tokyo, 100-8370, Japan

**Keywords:** Optical Parametric Amplification, Microstructured Optical Fiber, Chromatic Dispersion Control.

**Abstract:** The performance of fiber-optical parametric amplification is studied by employing the AsSe<sub>2</sub>-based hybrid microstructured optical fiber (HMOF). By adding a buffer layer around the core with appropriate diameter and refractive index difference, the chromatic dispersion profile of chalcogenide HMOFs can be tailored to have a near-zero and flattened anomalous dispersion regime in the mid-infrared window. A very broad gain bandwidth can be achieved from 3.0 to 9.0  $\mu\text{m}$  by pumping at 4.7  $\mu\text{m}$ . The signal gain can be as high as 32 dB. In addition, the HMOF with buffer layer can suppress the chromatic dispersion variation caused by the fiber structure fluctuation and maintain the signal gain spectrum.

## 1 INTRODUCTION

Fiber optical parametric amplification (FOPA) has attracted much attention since it can provide high signal gain and broad gain bandwidth in the wavelength range where other types of amplifiers such as Erbium-doped fiber amplifiers (EDFAs) and fiber Raman amplifiers (RAs) can't reach. Their potential applications are not only for high-speed and long-haul transmission systems, but also for ultrafast all-optical signal processing, pulse regeneration, optical time-division demultiplexing, optical sampling, quantum noise and correlation (M. E. Marhic, 2008). By expanding the wavelength range of FOPA gain bandwidth towards the mid-infrared region which exceeds the transparency limit of fused-silica fibers, more interesting applications in spectroscopy, sensing, biology and metrology can be realized. However, it is still a challenging task.

Recently, many non-silica glasses such as tellurite glasses (Domachuk et al., 2008, Liao et al., 2009), heavy metal fluoride glasses (Xia et al., 2009, Qin et al., 2009) and chalcogenide glasses (Mouawad et al., 2014, Petersen et al., 2014) have been demonstrated as alternative candidates. Among them, chalcogenide glasses have very broad transmission window up to 10  $\mu\text{m}$  and very high nonlinearities in comparison

with silica. But, the use of chalcogenide fibers suffers from the large normal dispersion in the infrared window, which dramatically reduces the efficiency of FOPA performance. The zero dispersion wavelengths (ZDWs) of chalcogenide fibers are commonly located far away from the operating wavelengths of commercially available laser sources. It leads to the difficulty in pumping those fibers in the anomalous dispersion region.

In this work, we propose AsSe<sub>2</sub>-based hybrid microstructured optical fibers (HMOFs) (Tong et al., 2013) with controlled chromatic dispersion profiles. By employing the brilliant properties of chalcogenide glass, and the control of near-zero and flattened chromatic dispersion profile of HMOFs, it is expected to achieve a novel performance of FOPA in the mid-infrared window.

## 2 CHROMATIC DISPERSION AND PARAMETRIC GAIN CALCULATION

A commercial full-vectorial mode solver (Lumerical-Mode Solution software) based on the finite element method and the perfectly matched layer boundary condition was used to calculate the chromatic

dispersion profiles of the proposed chalcogenide fibers.

The core material is the AsSe<sub>2</sub> glass which is made by Furukawa Denshi company. Its refractive indices at 20 wavelengths from 0.4 to 4.0 μm were measured by using the glass prism and the minimum deviation method (Werner, 1968). The fiber cladding material was designed in order that the refractive index difference (Δn) between core and cladding materials is equal to 0.3. The refractive index profiles of both core and cladding materials were input into the Mode Solution software as initial parameters.

The calculation of parametric gain in this work has based on the theory of the degenerate four-wave mixing process whose phase-matching condition is given by (G. P. Agrawal, 2007)

$$\kappa = \Delta\beta + 2\gamma P \quad (1)$$

where  $P$  is the pump power,  $\gamma$  is the nonlinear coefficient and the linear phase-mismatch  $\Delta\beta$  is expressed by (G. P. Agrawal, 2007)

$$\begin{aligned} \Delta\beta &= \beta_i + \beta_s - 2\beta_p \\ &= \frac{n_{eff}(\omega_i)\omega_i}{c} + \frac{n_{eff}(\omega_s)\omega_s}{c} - \frac{2n_{eff}(\omega_p)\omega_p}{c} \end{aligned} \quad (2)$$

The effective refractive indices at the frequencies of the pump  $\omega_p$ , signal  $\omega_s$  and idler  $\omega_i$  are  $n_{eff}(\omega)$ ,  $n_{eff}(\omega_s)$  and  $n_{eff}(\omega_i)$ , respectively.

Commonly, the linear phase-mismatch  $\Delta\beta$  is calculated by using the second and fourth terms of the Taylor series expansion. But in this work,  $\Delta\beta$  is fully calculated by using the frequency dependent effective refractive index  $n_{eff}(\omega)$  obtained from Mode solution software. For this reason, the contributions of higher order dispersion parameters ( $\beta_6, \beta_8, \dots$ ) are taken into account to improve the accuracy of the phase matching condition and FOPA gain.

The optical signal gain ( $G_s$ ) is given by (Hansryd et al., 2002)

$$G_s = \frac{P_s(L)}{P_s(0)} = 1 + \left(\frac{\gamma P}{g}\right)^2 \sinh^2(gL) \quad (3)$$

where  $L$  is the fiber length,  $P_s(0)$  and  $P_s(L)$  are the signal power at the input and output of the fiber. The parametric gain coefficient  $g$  is given by (Hansryd et al., 2002).

$$g = \sqrt{(\gamma P)^2 - \left(\frac{\kappa}{2}\right)^2} = \sqrt{(\gamma P)^2 - \left(\gamma P + \frac{\Delta\beta}{2}\right)^2} \quad (4)$$

### 3 RESULTS AND DISCUSSIONS

The conventional step index was first designed and its structure is shown in Fig. 1a. The diameter of the AsSe<sub>2</sub> core was 2.0 μm. The chromatic dispersion profile of the fundamental mode was calculated within the wavelength range from 2.0 to 11.0 μm and is shown in Fig. 1b. As can be seen, only normal dispersion region was obtained from 2.0 to 8.1 μm. At the wavelengths larger than 8.1 μm, the modal confinement was so weak that no mode could be found in the core.

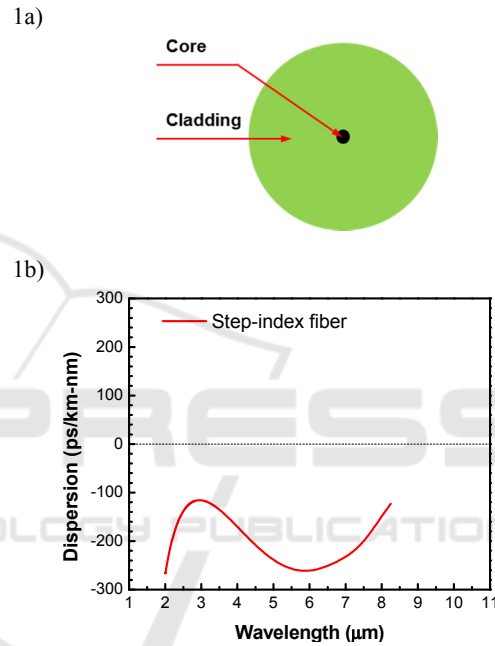


Figure 1: a) Fiber structure of an AsSe<sub>2</sub> step-index fiber and b) its calculated chromatic dispersion profile of the fundamental mode.

In order to enhance the modal confinement in the core, a ring of six air holes with hexagonal structure was designed in the cladding region. The diameter of the AsSe<sub>2</sub> core was still 2.0 μm. The diameter of each air hole was 4.0 μm and the pitch which is the distance between two adjacent air holes was 7.0 μm. This fiber structure is shown in Fig. 2a and is named as a hybrid microstructured optical fiber. The chromatic dispersion profile of the fundamental mode was calculated and is shown in Fig. 2b. In comparison with the conventional AsSe<sub>2</sub> step index fiber, the AsSe<sub>2</sub> HMOF could support the fundamental mode at wavelengths longer than 8.1 μm. The zero-dispersion wavelength was found at 10.1 μm. The anomalous dispersion regime was realized at wavelengths over 10.1 μm.

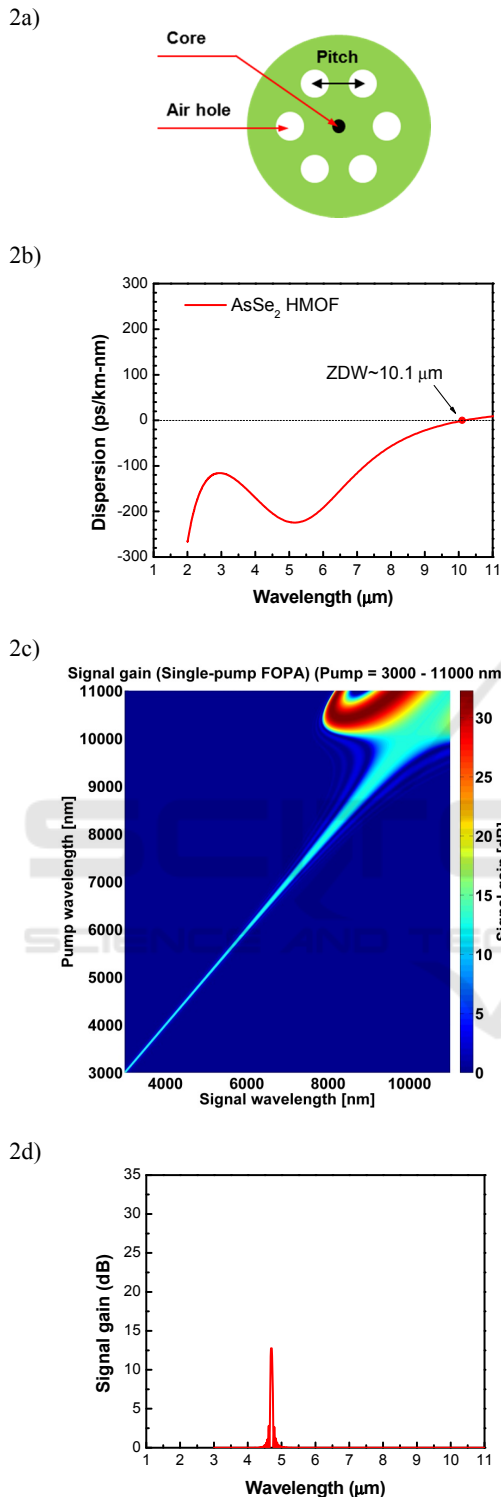


Figure 2: a) Fiber structure of an AsSe<sub>2</sub> HMOF, b) its calculated chromatic dispersion profile of the fundamental mode, c) signal gain map obtained by pumping the AsSe<sub>2</sub> HMOF at different pump wavelengths from 3.0 to 11.0 μm and d) calculated signal gain spectrum obtained by pumping at 4.7 μm.

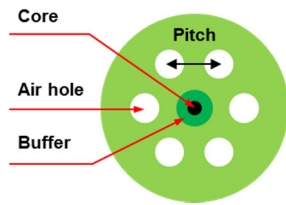
The calculation of FOPA signal gain was carried out by using the chromatic dispersion profile of the AsSe<sub>2</sub> HMOF in Fig. 2b. The fiber length was 3 cm. The pump power was 3 W and the nonlinear coefficient was supposed to be  $4.9 \times 10^4 \text{ W}^{-1}\text{km}^{-1}$  (Cheng et al., 2014). The FOPA performance was investigated when the pump and signal wavelengths varied from 3.0 to 11.0 μm. Figure 2c shows the signal gain map in which the colour scale expresses the intensity of the signal gain. At different pump wavelength, the gain bandwidth can be estimated from the horizontal dimension of the signal gain map. Figure 2c depicts that FOPA gain bandwidth is very narrow when the pump wavelength is from 3.0 to about 9.0 μm. For instance, the FOPA signal gain and bandwidth is calculated and shown in Fig. 2d when the pump wavelength is at 4.7 μm. But, the gain bandwidth increases when the pump wavelength becomes closer to the ZDW (10.1 μm) as shown in Fig. 2c. When the pump wavelength locates in the anomalous dispersion regime, both of signal gain and bandwidth improve greatly. This feature implies that the anomalous dispersion regime should be realized at shorter wavelengths because it is not easy to pump the fiber at wavelengths over 10 μm by several commercially available laser sources at this time.

To obtain the anomalous dispersion regime in the shorter wavelength range, a new fiber structure of AsSe<sub>2</sub> HMOF was proposed. A new layer of material which is called as the buffer layer was added around the core. By changing the diameter of the buffer and the  $\Delta n$  between the buffer and core materials, the chromatic dispersion profile of the original HMOF can be modified. In Fig. 3a, the buffer layer whose diameter is 5.2 μm was added. The  $\Delta n$  between the buffer and core is equal to 0.02.

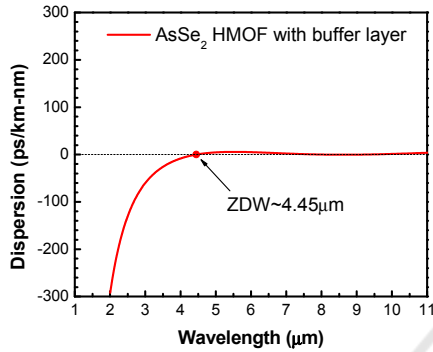
The properties of chromatic dispersion, signal gain map and signal gain spectrum for the AsSe<sub>2</sub> HMOF with the buffer layer are shown in Fig. 3. They are totally different from those of the original AsSe<sub>2</sub> HMOF shown in Fig. 2. The anomalous dispersion regime was obtained from 4.45 to 11.00 μm. It is very close to zero and flattened. The ZDW was shifted from 10.0 to 4.45 μm. The new FOPA performance shown in Fig. 3c is consistent with the discussions for Fig. 2c. When the pump wavelength is close to the ZDW and locates in the anomalous dispersion regime, a very broad gain bandwidth can be realized. Figure 3d shows the signal gain spectrum when the pump wavelength is 4.7 μm. The signal gain can be as high as 32 dB. At 12 dB, a broad gain bandwidth about 6500 nm was obtained. It is much broader than the 1000-nm bandwidth near 2.94 μm simulated by using a 20-cm-long chalcogenide step-index fiber

with 20-W CW pump (Singh et al., 2012).

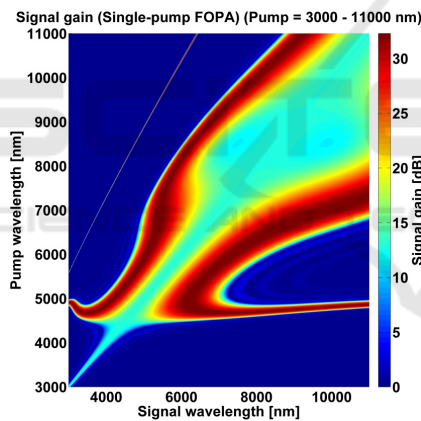
3a)



3b)



3c)



3d)

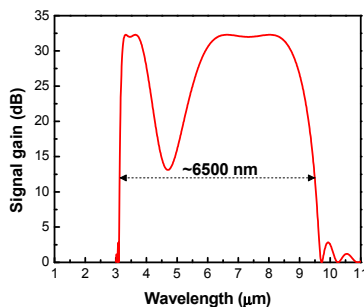
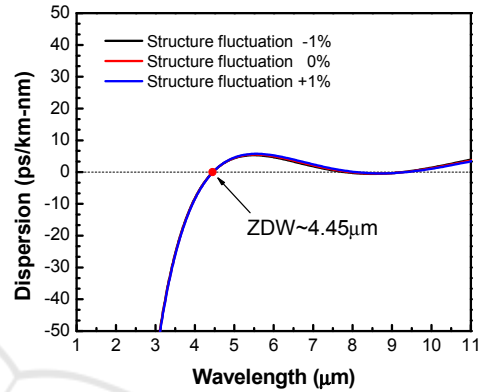


Figure 3: a) Fiber structure of an AsSe<sub>2</sub> HMOF with a buffer layer, b) its calculated chromatic dispersion profile of the fundamental mode, c) signal gain map obtained by pumping the AsSe<sub>2</sub> HMOF with a buffer layer at different pump wavelength from 3.0 to 11.0 μm and d) calculated signal gain spectrum obtained by pumping at 4.7 μm.

In addition, the effect of fiber structure variation was investigated in this work. The whole structure of the AsSe<sub>2</sub> HMOF with buffer layer was supposed to fluctuate by ±1%. However, the calculated chromatic dispersion was almost invariant to the fluctuation of fiber structure as shown in Fig. 4a. The shape of the signal gain spectrum was maintained in the wavelength range from 3.0 to 8.0 μm while the gain bandwidth slightly changed as shown in Fig. 4b.

a)



b)

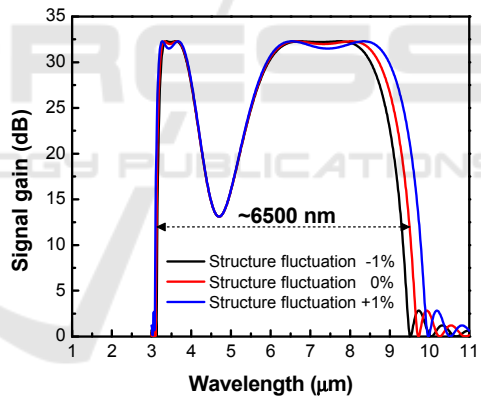


Figure 4: a) calculated chromatic dispersion profiles of the fundamental mode of the AsSe<sub>2</sub> HMOF and a buffer layer in Fig. 3a with ±1% fiber structure fluctuation and b) calculated signal gain spectra correspond to the chromatic dispersion profiles in Fig. 4a, obtained by pumping at 4.7 μm.

## 4 CONCLUSIONS

Chalcogenide HMOFs with a buffer layer are favourable for the performance of FOPA in the mid-infrared window. The advantages of wide transmission range, high nonlinearity, near-zero and flattened anomalous dispersion control by using chalcogenide HMOFs lead to a very broad FOPA

gain bandwidth and high signal gain. Moreover, it is very interesting that the chromatic dispersion can be invariant to the fiber structure fluctuation and the signal gain spectrum can be maintained.

## ACKNOWLEDGEMENTS

This work is supported by MEXT, the Support Program for Forming Strategic Research Infrastructure (2011-2015)

## REFERENCES

- M. E. Marhic, 2008. Fiber optical parametric amplifiers, oscillators and related devices, *Cambridge University Press*.
- P. Domachuk, N. A. Wolchover, M. Cronin-Golomb, A. Wang, A. K. George, C. M. B. Cordeiro, J. C. Knight and F. G. Omenetto, 2008. Over 4000 nm Bandwidth of Mid-IR Supercontinuum Generation in sub-centimeter Segments of Highly Nonlinear Tellurite PCFs, *Opt. Express*, 16, 7161-7168.
- M. Liao, X. Yan, G. Qin, C. Chaudhari, T. Suzuki and Y. Ohishi, 2009. A highly non-linear tellurite microstructure fiber with multi-ring holes for supercontinuum generation, *Opt. Express*, 17, 15481-15490.
- C. Xia, Z. Xu, M. N. Islam, F. L. Terry, M. J. Freeman, A. Zakel and J. Mauricio, 2009. 10.5 W time-averaged power mid-IR supercontinuum generation extending beyond 4  $\mu\text{m}$  with direct pulse pattern modulation, *IEEE J. Sel. Top. Quantum Electron.*, 15, 422-434.
- G. Qin, X. Yan, C. Kito, M. Liao, C. Chaudhari, T. Suzuki and Y. Ohishi, 2009. Ultrabroadband supercontinuum generation from ultraviolet to 6.28  $\mu\text{m}$  in a fluoride fiber, *Appl. Phys. Lett.*, 95, 161103.
- Mouawad, J. Picot-Clémente, F. Amrani, C. Strutynski, J. Fatome, B. Kibler, F. Désévéday, G. Gadret, J. C. Jules, D. Deng, Y. Ohishi and F. Smektala, 2014. Multioctave midinfrared supercontinuum generation in suspended-core chalcogenide fibers, *Opt. Lett.*, 39, 2684-2687.
- C. R. Petersen, U. Møller, I. Kubat, B. Zhou, S. Dupont, J. Ramsay, T. Benson, S. Sujecki, N. Abdel-Moneim, Z. Tang, D. Furniss, A. Seddon and O. Bang, 2014. Mid-infrared supercontinuum covering the 1.4–13.3  $\mu\text{m}$  molecular fingerprint region using ultra-high NA chalcogenide step-index fibre, *Nat. Photonics*, 8, 830-834.
- H. T. Tong, T. Cheng, K. Asano, Z. Duan, W. Gao, D. Deng, T. Suzuki, and Y. Ohishi, 2013. Optical parametric gain and bandwidth in highly nonlinear tellurite hybrid microstructured optical fiber with four zero-dispersion wavelengths, *Opt. Express* 21, 17, 20303-20312.
- J. Werner, 1968. Methods in High Precision Refractometry of Optical Glasses, *Appl. Optics*, 7, (5), 837-843.
- G. P. Agrawal, 2007. Nonlinear fiber optics, Amsterdam, London, Elsevier/Academic Press.
- J. Hansryd, P. A. Andrekson, M. Westlund, J. Li, and P. O. Hedekvist, 2002. Fiber-based optical parametric amplifiers and their applications, *IEEE J. Sel. Top. Quant.*, 8, 506-520.
- T. Cheng, Y. Kanou, D. Deng, X. Xue, M. Matsumoto, T. Misumi, T. Suzuki, and Y. Ohishi, 2014. Fabrication and characterization of a hybrid four-hole AsSe<sub>2</sub>-As<sub>2</sub>S<sub>5</sub> microstructured optical fiber with a large refractive index difference, *Opt. Express*, 22, 13322-13329.
- S. P. Singh, S. K. Varshney, and P. K. Datta, 2012. Optical Parametric Amplification in Chalcogenide Step Index Fiber over Infrared Region, International Conference on Fibre Optics and Photonics, *OSA Technical Digest (online) (Optical Society of America, 2012)*, paper WPO.12.